

# Rule based system for archaeological pottery classification ☆

Martin Kampel \*, Robert Sablatnig

*Vienna University of Technology, Institute of Computer Aided Automation, Pattern Recognition and Image Processing Group 183/2,  
Favoritenstr. 9, A-1040 Wien, Austria*

Available online 5 October 2006

## Abstract

Motivated by the requirements of the present archaeology, we are developing an automated system for archaeological classification of ceramics. Classification and reconstruction of archaeological fragments is based on the profile, which is the cross-section of the fragment in the direction of the rotational axis of symmetry. In order to segment the profile into primitives like rim, wall, and base, rules based on human expert knowledge are created. The input data for the estimation of the profile is a set of points produced by the acquisition system. A function fitting this set is constructed and later on processed to find the characteristic points necessary to classify the original fragment. We demonstrate the method and give results on real archaeological data.

© 2006 Elsevier B.V. All rights reserved.

**Keywords:** Archaeological ceramics; Typology and classification; Curvature analysis; 3D acquisition

## 1. Introduction

Ceramics are one of the most widespread archaeological finds and are a short-lived material. This property helps researchers to document changes of style and ornaments. Therefore, ceramics are used to distinguish between chronological and ethnic groups. Furthermore ceramics are used in the economic history to show trading routes and cultural relationships. Especially ceramic vessels, where shape and decoration are exposed to constantly changing fashion, not only allow a basis for dating the archaeological strata, but also provide evidence of local production and trade relations of a community as well as the consumer behavior of the local population (Orton et al., 1993).

In order to make a later classification possible, the object is described in different ways: shape, decoration,

technological manufacturing stage, material, and color. Shape is usually described in terms of type-series using traditional pottery classification systems. For this, the description of the profile is important. Decoration, material, color, and a careful examination of the traces left on the vessel which indicate the steps taken during the manufacturing process is a further important property to be investigated in order to perform a subsequent classification.

All descriptions of the object serve only one final aim: the correct *classification* of the material. There are several different ways of classifying vessels: based on their shape, rim form, the presence of handles or spouts, decorative motifs and so on. The purpose of classification is not only to get a systematic view of the material found but also to find different fragments belonging to the same vessel based on attributes stored in an archive database. After that, the profile of the fragment can be used to reconstruct the original (complete) vessel. This includes the possibility of reconstructing missing parts of the vessel and the search for possible matches of other fragments already stored in the archive with the one that is under consideration (part-assembly).

Up to now all this has been done manually which means a lot of routine work for archaeologists and a very

☆ This work was partly supported by the Austrian Science Foundation (FWF) under grant P13385-INF, the European Union under grant IST-1999-20273 and Culture and by the innovative project '3D technology' of the Vienna University of Technology.

\* Corresponding author. Tel.: +43 15880118364.

E-mail addresses: [kampel@prip.tuwien.ac.at](mailto:kampel@prip.tuwien.ac.at) (M. Kampel), [sab@prip.tuwien.ac.at](mailto:sab@prip.tuwien.ac.at) (R. Sablatnig).

URL: [www.prip.tuwien.ac.at](http://www.prip.tuwien.ac.at) (M. Kampel).

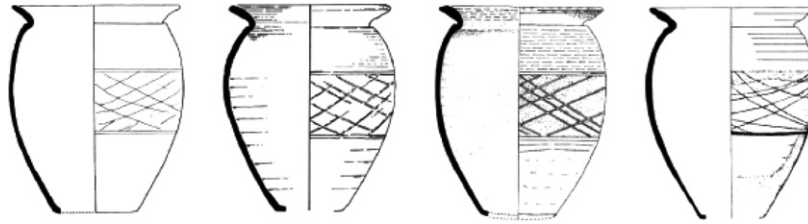


Fig. 1. The limits of objective recording: the same vessel drawn by four different illustrators (from Orton et al., 1993).

inconsistent representation of the real object (Orton et al., 1993). First, there may be errors in the measuring process, diameter or height may be inaccurate, second, the drawing of the fragment should be in a consistent style, which is not possible since a drawing of an object without interpreting it is very hard to do. The third process, grouping or classifying, is also a very difficult task.

There have been several attempts to develop a reliable method of classification (Binford, 1965; Adams and Adams, 1991; Sinopoli, 1991), none of which is widely accepted. A graphic documentation done by hand additionally raises the possibility of errors. This leads to a lack of objectivity in the documentation of the material found. To give an example, a vessel was drawn by four different illustrators resulting in four different vessels as shown in Fig. 1. Note the different shape and decoration, the rim and the thickness for instance are significantly different.

Gilboa et al. (2004) presents a strategy that pertains to typology and classification which are confined to shape attributes. Their analysis is based on the description of a planar curve in terms of its curvature function. Their main source of error is that the information is derived from hand drawn profiles, whose accuracy cannot be assessed. Here we use digitized information for extracting quantitative measures for various measures of the profile.

This paper is organized as follows. In Section 2, we describe the acquisition method for 3D-shape estimation and how we estimate the profile sections. Next we show the determination of shape characteristics based on so-called characteristic points in Section 3. The generation of primitives is presented in Section 4. Results using real archaeological data are given in Section 5, followed by conclusions and outlook on future work.

## 2. Data acquisition

The acquisition method for estimating the 3D-shape of a fragment is shape from structured light (DePiero and Trivedi, 1996), which is based on active triangulation (Besl, 1988). We used the *Vivid 900* 3D Scanner developed by MINOLTA.<sup>1</sup>

Fig. 2 illustrates the acquisition setup consisting of the Vivid 900 Scanner connected to a PC and the object to be recorded. Optionally the object is placed on a turntable

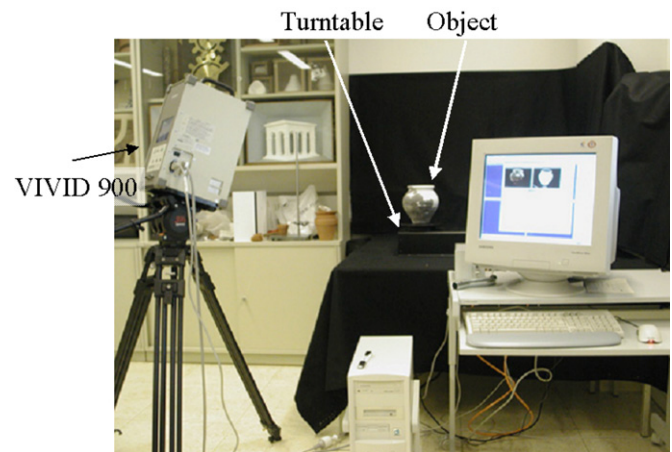


Fig. 2. The Minolta VIVID 900 Scanner.

with a diameter of 40 cm, whose desired position can be specified with an accuracy of  $0.1^\circ$ . The 3D Scanner works on the principle of laser triangulation combined with a color CCD image. It is based on a laser-stripe but a galvanometer mirror is used to scan the line over the object.

We have carried out in situ tests to capture 3D sherds and other finds from the excavation site CARNUNTUM (Gruenewald, 1986) in Austria. For each fragment two views (front- and back-views) have been recorded. Common sizes of fragments range from  $10 \times 10 \times 8$  cm to  $30 \times 30 \times 20$  cm, and they are recorded with an accuracy of 0.5 mm. The 3D-data is stored as a software independent *VRML*-file containing 3D-points that are connected in form of triangles. Our pottery dataset currently consists of 40 different sherds.

Archaeological pottery is assumed to be rotationally symmetric since it was made on a rotation plate. With respect to this property the axis of rotation is calculated using a Hough inspired method (Sablatnig and Kampel, 2002). To perform the registration of the two surfaces of one fragment, we use a priori information about fragments belonging to a complete vessel: both surfaces have the same axis of rotation since they belong to the same object. Consequently, we register the two views by calculating the axis of rotation and by bringing the resulting axes into alignment. A detailed description of the registration algorithm can be found in (Sablatnig and Kampel, 2002). The technique proposed works best for wheel-thrown pottery, and would not be suitable for hand-made pottery, since it relies on the rotational symmetry.

<sup>1</sup> MINOLTA Austria GMBH: [www.minolta.com](http://www.minolta.com).

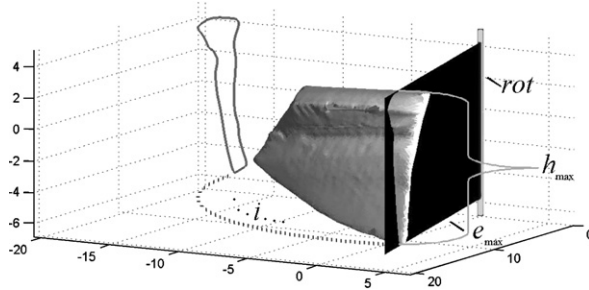


Fig. 3. Orientated sherd, rotational axis, intersecting plane  $e_{\max}$  and longest profile line.

The registration of front- and back-view together with the axis of rotation provide the profile used to reconstruct the vessel.

Fig. 3 shows the 3D-model of a sherd and its rotational axis  $rot$  as a vertical line along the  $z$ -axis. The black plane represents the intersecting plane  $e_{\max}$  at the maximum height  $h_{\max}$  of the sherd. The longest profile line is the longest line along the surface of the sherd parallel to the rotational axis  $rot$ . The radius  $r$  is the estimated mean radius of the profile line. The extracted profile line is shown in the  $xz$ -plane. Our algorithm for the estimation of the longest profile line consists of the following steps:

- (1) First the axis of rotation is transformed into the  $z$ -axis of the coordinate system in order to simplify further computation.
- (2) The fragment's size described by its circular arc is estimated. Depending on the size we compute a number of intersecting planes  $e_i$ , which are used for the profile estimation. The number of planes  $e_i$  depends on the length of the perimeter of the fragment. Experiments have shown that 7–13 profile lines return the best ratio of exactness and performance. Fig. 4 shows a sample of four planes  $e_i$  intersecting the 3D-model and the plots of the extracted profile lines on the surface of the sherd.

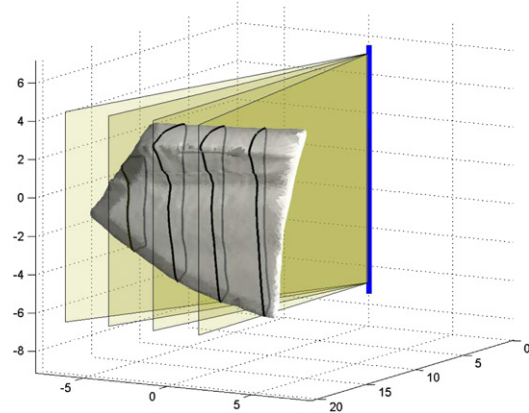


Fig. 4. Sample of intersecting planes  $e_i$ .

- (3) A profile line is calculated by intersecting the 3D-data of the fragment with planes  $e_i$ : first the distance of each vertex of the fragment to the plane  $e_i$  is calculated. All vertices are sorted by their distance to the plane. Then the nearest 1% of vertices are selected as candidates for the profile. The result is a properly oriented profile line.
- (4) Next the profile line having the longest line is found: the difference between the maximum  $z$ -value and the minimum  $z$ -value of the profile line defines the height of the profile line. The remaining profile lines are used for evaluation of the estimate of the rotational axis.

Fig. 5 shows two plots of diameters based on the profiles from two different fragments. The  $y$ -axis is the difference of the diameters to the overall mean diameter of all profiles in centimeters and the  $x$ -axis corresponds to the circular arc. The upper line shows the maximum diameter, the middle shows the mean diameter and the lower line shows the minimum diameter. The grey box allows the quality of the results to be visualized by showing the overall mean diameter of all profiles versus the standard deviation of all profiles. If the standard deviation exceeds a certain threshold

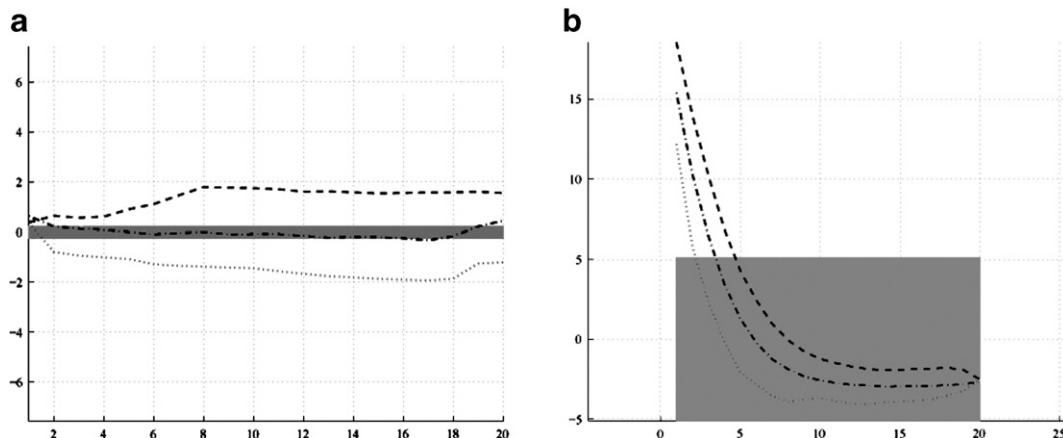


Fig. 5. Maximum, mean and minimum diameters.

(for example 0.5 cm) the fragment is excluded from further reconstruction.

As can be seen in Fig. 5a a correctly estimated rotational axis results in mean diameter with a small standard deviation (smaller than 0.5 cm) along the perimeter of the sherd. Also the minimum and the maximum diameter are constant except on the left and right side, where the fracture of the fragment is located. In Fig. 5b the mean diameter along the perimeter has a standard deviation of more than 0.5 cm (in this case 5 cm). This indicates that the estimate of the rotational axis is not accurate enough for further processing. In this case, we plan to extend the algorithm for axis estimation by using additional information on the fragment e.g. rills on the inner surface, detection of rim-fragments.

Experiments were done on all 40 fragments of our pottery database. The success rate for correct extraction of the profile line and consequently the percentage of sherds used for further reconstruction is around 50% of the data found at the excavation site. This should be compared to manual archivation done by archaeologists (Orton et al., 1993): for coarse ware around 35% (Degeest, 2000) and for fine ware around 50% (Poblome, 1999) of the findings are used for further classification. It depends heavily on the shape of the fragment (e.g. handle, flat fragments like bottom pieces, small size, etc.). Eighteen fragments have been excluded from reconstruction due to incorrect estimation of the axis of rotation. Details on the evaluation can be found in (Kampel and Sablatnig, 2003).

### 3. Determination of shape characteristics

By classifying the parts of the profile, the complete vessel is classified, and missing parts may be reconstructed. Following the manual strategy of the archaeologists, the profile should first be automatically segmented into its parts, the so-called *primitives* (Kampel and Sablatnig, 2002). Our approach to do so is a hierarchical segmentation of the profile into rim, wall, and base by creating segmentation rules based on expert knowledge of the archaeologists and the curvature of the profile. These three segments of the profile are stored in a so-called *description* of the profile. Fig. 6 shows an archive drawing of a frag-

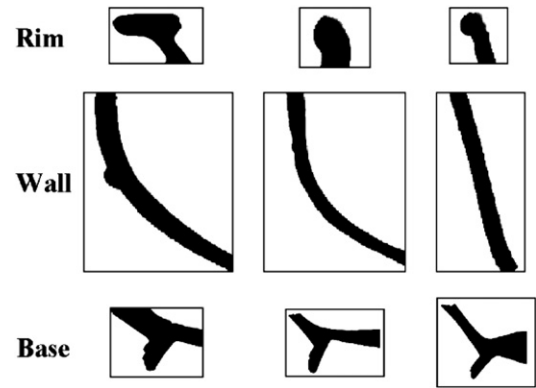


Fig. 7. Different shapes of primitives.

ment with its profile section divided into various primitives. If there is a corner point, that is a point at which the curvature changes “substantially”, the segmentation point is obvious. If there is no corner point, the segmentation point has to be determined mathematically (Adams and Adams, 1991).

Up to now this segmentation has been done manually by archaeologists, and there are no segmentation standards in archaeology (Adams and Adams, 1991). Fig. 7 shows different shapes of manually segmented primitives.

The basis for the segmentation is the outer profile line, i.e. the profile line along the outside of the vessel. The segments of the profile are divided by so-called characteristic points or segmentation points. Fig. 8 shows the classification scheme applied to an “S-shaped vessel” as an example. The coordinate system has its origin at the intersection point of the axis of rotation and the orifice line.

In order to allow proper segmentation, the following points have been identified.

- SP, starting point: in the case of vessels with a horizontal rim: innermost point, where the profile line touches the orifice plane.
- OP, orifice point: outermost point, where the profile line touches the orifice plane.
- IP, inflexion point: point, where the curvature changes its sign, i.e. where the curve changes from a left turn to a right turn or vice versa.

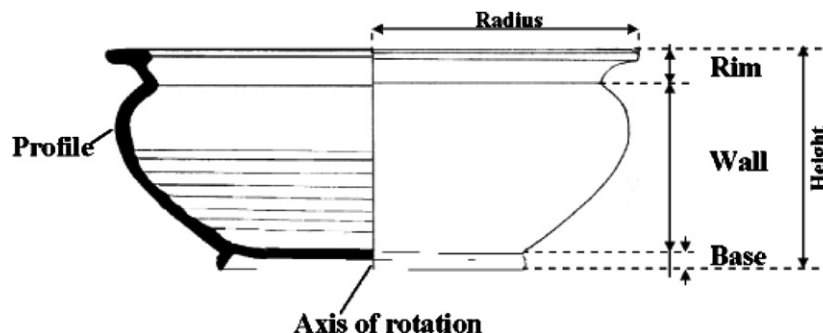


Fig. 6. Profile with known primitives.



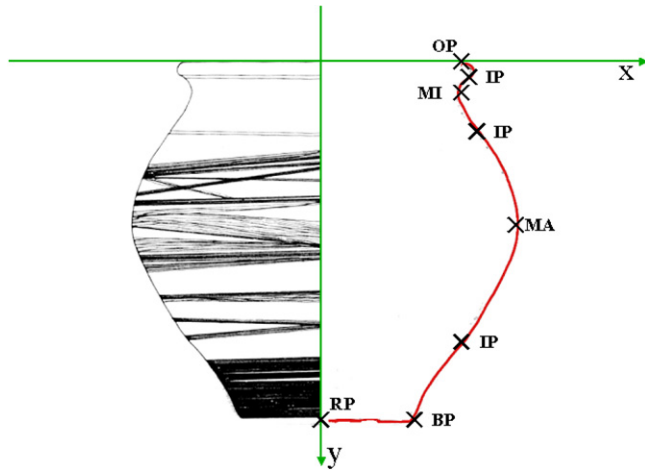


Fig. 8. S-shaped vessel: profile segmentation scheme.

- MI, local minimum: point of vertical tangency; point where the  $x$ -value is smaller than in the surrounding area of the curve.
- MA, local maximum: point of vertical tangency; point where the  $x$ -value is bigger than in the surrounding area of the curve; the  $y$ -value refers to the height of the object (e.g.  $MA(y)$ ).
- CP, corner point: point where the curve changes its direction substantially.
- BP, base point: outermost point, where the profile line touches the base plane.
- RP, point of the axis of rotation: point where the profile line touches the axis of rotation.
- EP, end point: point where the profile line touches the axis of rotation; applied to incomplete profiles.

The profile determined has to be converted into a parameterized curve (Hu and Ma, 1995) and the curvature has to be computed (Bennett and MacDonald, 1975). Local changes in curvature (Rosenfeld and Nakamura, 1997) are the basis for rules required for segmenting the profile. Based on the B-spline methods (Hall and Laffin, 1984) the profile is thus converted into one or more mathematical curves.

In order to apply interpolation and approximation methods the profile is subdivided into sub-intervals by using corner points. The most appropriate interpolation and approximation methods are computed and selected for each of the intervals of the curve, the method with a smaller error (in case of ambiguity, the interpolation method is preferred) is selected for the interval. The approximation error of the representation over the whole curve is computed via the sum of squares of the differences of the input value and the spline value. The situation is complicated by the fact that ceramic vessels, produced by hand, do not have mathematically perfect surfaces which affects the application of the above mentioned methods. Consequently, the precision of the representation of the vessels is reduced (Rice, 1987). The technique applied is thoroughly described in (Kampel and Sablatnig, 2002).

#### 4. Generation of primitives

The attributes of a successful classification have been summarized by Orton et al. (1993):

- objects belonging to the same type should be similar (internal cohesion),
- objects belonging to different types should be dissimilar (external isolation),
- the types should be defined with sufficient precision to allow others to duplicate the classification,
- it should be possible to decide to which type a new object belongs.

In order to achieve these aims our classification scheme of the vessel form is based on two aspects (Orton et al., 1993):

- absolute measurements and ratios,
- segmentation of the profile line.

The first step is the measurement of the following parameters: rim diameter, bottom diameter, height,  $x$ - and  $y$ -values of all segmentation points. With these measurements a variety of ratios can be calculated. A specific choice of these ratios is in each case characteristic for one vessel type; for example the ratio rim diameter to the height of the fragment.

The characteristic points together with the following measurements are used to define basic vessel forms and types (Andraschko et al., 1990):

- Rim-diameter,  $rdm$ : The diameter of the orifice plane.
- Wall-diameter,  $wdm$ : The maximum diameter of the object orthogonal to its rotational axis.
- Bottom-diameter,  $bdm$ : Diameter at the bottom of the object.
- Height,  $h$ : The overall height of the object.
- The characteristic ratio,  $r_{chr}$ : The ratio between height  $h$  and rim-diameter  $rdm$ :  $h:rdm$ .

Together with archaeologists (Adler et al., 2001) three levels of hierarchical classification rules based on the work of Schreg (1978) and Andraschko et al. (1990) have been worked out. They consist of three consecutive levels *ware*, *basic form* and *basic type*, see Table 1. These rules were applied to the late Roman burnished ware of Carnuntum (Gruenewald, 1986). The first classification level defines the fabric or pottery ware.

Table 1  
Three levels of classification

I	Ware	Late Roman burnished ware
II	Basic form	Beaker, plate, bowl, pot, jug
III	Basic type	Beaker1, beaker2, pot1, pot2, plate1–2, plate11–2, plate13–7, jug1, jug2–3, jug4

Table 2  
Classification level II: specific vessel forms











Basic vessel form	$r_{chr}$ ( $\pm 15\%$ )	$rdm$ (cm)	$wdm$ (cm)
Plate	1:8	16–34	–
Bowl	1:2–1:4	10–16	–
		12–30	–
Beaker	1:1	8–11	5–14
Jug	4:1–2:1	6–14	–
Pot	1:1–3:1	8–12	15–25
		12–16	18–21

Classification level II defines *basic forms* (see Table 2). The grouping follows functional aspects based on characteristic ratios and diameter. A variation of  $\pm 15\%$  is taken

into account. For example, a plate is defined by  $r_{chr} = 1:8$  and  $rdm$  ranging from 16 cm to 34 cm.

The forms are subdivided into *basic vessel types* (see Table 3), which are defined in level III. The grouping follows the characteristic properties of the profile section and the position of the characteristic points. Table 3 shows the rules and images of all vessel types which are taken into account ( $a \gg b$  means at least 20% difference between  $a$  and  $b$ ). These rules were found empirically and are only valid for the specific ware. References of all forms to Gruenewald (1986) and representative images of the specific form are given. For example, a plate is further specified by not having an inflection point IP and no curvature point CP.

Table 3  
Classification level III: basic vessel types

Basic vessel types	Characteristic points	Characteristic properties of the profile section	Reference (Gruenewald, 1986)	Image
Beaker1	1 IP, no CP	$rdm \gg bdm$	78/1–4	
Beaker2	>1 IP	$rdm \approx wdm$	78/6	
Plate1–2	1 IP, no CP	$f(x+1) > f(x)$	71/9; 75/1–4	
Bowl1–2	1 IP, no CP	$f(x+1) \geq f(x)$ , $MA(y) < \frac{h}{10}$	70/1–6; 71/2	
Bowl3–7	CP, >1 IP	$f(x+1) \gg f(x)$	72/5–8; 73/1–3; 74/4, 6–8	
Pot1	>1 IP	$rdm \geq bdm$ , $rdm \ll wdm$ , $MA(y) > \frac{h}{5}$	79/2; 81/2	
Pot2	1 IP, no CP	$rdm \ll wdm$ , $MA(y) \cong \frac{h}{2}$	79/1, 3	
Jug1	>1 IP	$rdm < wdm$ , $wdm \gg bdm$	–	
Jug2–3	CP	$rdm \approx bdm$	84/10	
Jug4	>1 IP or CP	$rdm < 12$ cm	84/1–3, 8; 85/2–7, 9–11	

## 5. Results

First we show results of finding characteristic points using the multi-spline method. Next we present experiments on the segmentation of the characteristic points, which is followed by examples of automatic classification. The pottery dataset used for the experiments was already classified by archaeologists and published by Gruenewald (1986). Besides the manual drawings of the fragments, the fragments themselves were available. In order to evaluate the classification results achieved, we randomly selected eight fragments from the pottery dataset, classified them, and compared the results to manual classification results of the same fragments.

Following the manual approach of the archaeologists, we take the outer profile line as basis for the segmentation: Fig. 9 shows two examples of automatically segmented pots with the characteristic points detected shown in (b), and the appropriate manual segmentation in (a).

Applying level II of the classification scheme to the curves computed gives a first indication of the group to which the object belongs. Table 4 summarizes results from eight fragments. The most important measurement is the diameter of the rim *rdm*, because its estimation does not depend on whether the object is a fragment or a vessel. On the contrary the diameter of the bottom *bdm* represents only a reliable indicator for vessels, because the *bdm* of a fragment is not the same as the *bdm* of the whole vessel.

For example, the *rdm* of fragment 70/1 is 15.6 cm, which allows the forms *plate*, *bowl* and *pot*. Its characteristic ratio  $r_{chr} = 1: < 1.5$  excludes *plates*, leading to *bowl* and *pot* as indication. Ambiguities are resolved within classification level III.

Table 5 shows results of the estimation of characteristic points. Except for IP, where the number of IPs found is shown, the coordinates of the characteristic points are given. One of the most reliable indicators is the number of IPs, because it identifies S-shaped forms by simply counting points without requiring of their position. The *y*-position of the MA characterizes forms reliably, because its approximate position is sufficient.

To continue the previous example with fragment 70/1, the forms *bowl* and *pot* are further investigated: the position of MA indicates that it is not a pot, since it lies within

Table 4

Classification level II: characteristic forms

ID (Gruenewald, 1986)	<i>rdm</i>	<i>wdm</i>	<i>bdm</i>	<i>h</i>	$r_{chr}$	Indication
70/1	15.6	19.2	9.2	10.2	1:1.5	Bowl, pot
70/4	19.6	21.6	9.6	6.4	1:3.0	Bowl
72/6	14.4	17.0	5.2	7.4	1:1.9	Bowl, pot
72/8	22.2	24.2	7.2	10.0	1:1.2	Bowl
75/3	29.6	32.4	16.2	5.6	1:5.3	Plate
78/2	6.4	7.2	4.6	9.2	1.4:1	Jug, pot, beaker
79/2	12	14.0	5.2	10.6	1:1.1	Pot, beaker
81/1	12.4	15.4	4.8	11.3	1:1.1	Beaker, pot

Table 5

Classification level III: characteristic types

ID	OP	MA	MI	# IP	CP	BP	RP	EP
70/1	[7.8, 0.0]	[9.6, 0.8]	EP	1	–	–	–	[4.6, 10.2]
70/4	[9.8, 0.0]	[10.8, 0.8]	BP	1	–	[4.8, 6.4]	–	–
72/6	[7.2, 0.0]	[8.5, 1.0]	EP	3	–	–	–	[2.6, 7.4]
72/8	[11.1, 0.0]	[12.1, 0.9]	EP	3	–	–	–	[3.6, 10.0]
75/3	[14.8, 0.0]	[16.2, 0.8]	BP	1	–	[8.1, 5.6]	–	–
78/2	[3.2, 0.0]	[3.6, 0.5]	EP	2	–	–	–	[2.3, 9.2]
79/2	[6.0, 0.0]	[7.0, 1.5]	EP	1	–	–	–	[2.6, 10.6]
81/1	[6.2, 0.0]	[7.7, 1.8]	EP	1	–	–	–	[2.4, 11.3]

the first 20% of the height *h*. Having 1 IP only gives priority to Bowl1–2, which actually is a correct classification (Gruenewald, 1986).

Table 6

Final classification

ID (Gruenewald, 1986)	Level II	Classification rules applied	Indication
70/1	Bowl, pot	1 IP, $MA(y) < \frac{h}{5} (\cong 0.8 < 2.0)$	Bowl1–2
70/4	Bowl	1 IP, $MA(y) < \frac{h}{5} (\cong 0.8 < 1.3)$	Bowl1–2
72/6	Bowl, pot	3 IP, $MA(y) < \frac{h}{5} (\cong 1.0 < 1.5)$	Bowl3/7
72/8	Bowl	3 IP, $MA(y) < \frac{h}{5} (\cong 0.9 < 2.0)$	Bowl3/7
75/3	Plate	1 IP	Plate1–2
78/2	Jug, pot	2 IP, $rdm > bdm; MA(y) < \frac{h}{5} (\cong 0.5 < 1.8)$	Beaker1
79/2	Pot, beaker	1 IP, $MA(y) < \frac{h}{5} (\cong 1.5 < 2.1)$	Pot1, pot2
81/1	Pot, beaker	1 IP, $MA(y) < \frac{h}{5} (\cong 1.8 < 2.3)$	Pot1, pot2

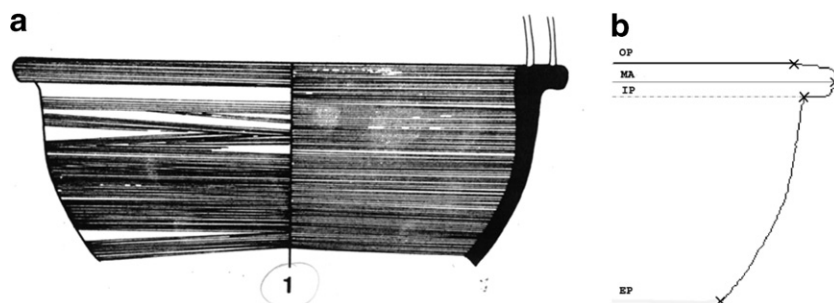


Fig. 9. Classified pottery 70/1: (a) manual drawings, (b) detected characteristic points.

Table 6 summarizes the results for the eight randomly selected fragments. The results achieved indicate the same basic vessel forms as published by Gruenewald (1986), except for 79/2 and 81/1. The reason is that distinction between forms pot1 and pot2 is not possible for fragments, where the bottom is missing, because it depends only on the relative position of MA.

## 6. Conclusion

In this paper, we presented the classification of the profile section based on the manual approach of the archaeologists. In order to define shape characteristics, a classification scheme was defined. The profile was segmented based on local changes in curvature, therefore B-Splines have been applied to the profiles. Three levels of classification based on characteristic measurements and the segmentation of the profile allowed the grouping of the fragment into specific vessel forms and specific vessel types. Results were shown for each intermediate step. The classification scheme presented depends on the excavation site. In order to apply our algorithm to other fragment-fabrics we have to redefine the classification scheme based on the characteristics of the specific fabric. Currently we are recording fragments at the excavation site Tel Dor in Israel. It is planned to apply our classification system on the resulting 3D-models (150–200 fragments).

## References

- Adams, W.Y., Adams, E.W., 1991. Archaeological Typology and Practical Reality. A Dialectical Approach to Artifact Classification and Sorting, Cambridge.
- Adler, K., Kampel, M., Kastler, R., Penz, M., Sablatnig, R., Hlavackova-Schindler, K., 2001. Computer aided classification of ceramics – achievements and problems. In: Börner, W., Dollhofer, L. (Eds.), Proc. 6th Internat. Workshop on Archaeology and Computers, Vienna, Austria, pp. 3–12.
- Andraschko, F.M., Krekeler, A., Schliep-Andraschko, N., 1990. Terminologie, Klassifikation und computergestützte Bearbeitung der Keramik des 1. Jahrtausends v. Chr. vom Westkom auf Elephantine, Oberägypten. In: Teegen, W.R., Andraschko, F.M. (Eds.), Gedenkschrift für Jürgen Driehaus, pp. 327–338.
- Bennett, J.R., MacDonald, J.S., 1975. On the measurement of curvature in a quantized environment. IEEE Trans. Comput. 24, 803–820.
- Besl, P.J., 1988. Active, optical range imaging sensors. Machine Vision Appl. 1 (2), 127–152.
- Binford, L.R., 1965. Archaeological systematics and the study of cultural process. Amer. Antiquity 31, 203–210.
- Degeest, R., 2000. The common wares of sagalassos. In: Walkens, M. (Ed.), Studies in Eastern Mediterranean Archaeology, III.
- DePiero, F., Trivedi, M., 1996. 3D computer vision using structured light: Design, calibration, and implementation issues. Adv. Comput.
- Gilboa, A., Karasik, A., Sharon, I., Smilansky, U., 2004. Towards computerized typology and classification of ceramics. J. Archaeol. Sci. 31, 681–694.
- Gruenewald, M., 1986. Ausgrabungen im Legionslager von Carnuntum (Grabungen 1969–1977). Der römische Limes in Österreich 34, 10–11.
- Hall, N.S., Laffin, S., 1984. A computer aided design technique for pottery profiles. In: Laffin, S. (Ed.), Computer Applications in Archaeology. Computer Center, University of Birmingham, Birmingham, pp. 178–188.
- Hu, Z., Ma, S.D., 1995. The three conditions of a good line parameterization. Pattern Recognition Lett. 16, 385–388.
- Kampel, Martin, Sablatnig, Robert., 2003. Profile based pottery reconstruction. In: Martin, D. (Ed.), Proc. IEEE/CVPR Workshop on Applications of Computer Vision in Archaeology, Madison, Wisconsin, USA, pp. CD-ROM.
- Kampel, M., Sablatnig, R., 2002. Automated Segmentation of archaeological profiles for classification. In: Kasturi, R., Laurendeau, D., Suen, C. (Eds.), Proc. 16th Internat. Conf. on Pattern Recognition, Quebec City, vol. 1. IEEE Computer Society, pp. 57–60.
- Orton, C., Tyers, P., Vince, A., 1993. Pottery in Archaeology. Cambridge University Press, Cambridge.
- Poblome, J., 1999. Sagalassos red slip ware. In: Walkens, M. (Ed.), Studies in Eastern Mediterranean Archaeology, II, Brepols.
- Rice, P.M., 1987. Pottery Analysis: A Sourcebook.
- Rosenfeld, A., Nakamura, A., 1997. Local deformations of digital curves. Pattern Recognition Lett. 18 (7), 613–620.
- Sablatnig, R., Kampel, M., 2002. Model-based registration of front- and backviews. Computer Vision and Image Understanding 87 (1), 90–103.
- Schreg, R., 1978. Keramik aus Südwestdeutschland. Eine Hilfe zur Beschreibung, Bestimmung und Datierung archäologischer Funde vom Neolithikum bis zur Neuzeit, Tübingen.
- Sinopoli, C.M., 1991. Approaches to Archaeological Ceramics, New York.